Preparation of arbitrary entangled quantum states of a trapped ion

B. Kneer[1,2] and C. K. Law[2]
[1] *Abteilung für Quantenphysik, Universität Ulm, D-89069 Ulm, Germany*
[2]*Rochester Theory Center for Optical Science and Engineering, and Department of Physics and Astronomy, University of Rochester, Rochester, New York 14627*
(Received 1 August 1997)

We present a scheme that deterministically generates an *arbitrary* prescribed quantum *entangled* state of a trapped ion. The quantum entanglement is between the external (center-of-mass motion in one dimension) and the internal (electronic) state of the trapped ion. We examine the influence of technical errors in our scheme. Further we show how to entangle the center-of-mass motion of the confined ion in two dimensions. [S1050-2947(98)02003-4]

PACS number(s): 42.50.Dv, 42.50.Vk, 32.80.Qk, 42.50.Lc

I. INTRODUCTION

A single trapped ion interacting with external electromagnetic fields is a rich and experimentally achievable quantum system that provides a physical basis for exploring various aspects of quantum mechanics, i.e., quantum entanglement [1,2]. Recently, there has been major progress in studying quantum state preparation in a Paul trap. This success is marked by the generation and detection of nonclassical states in experiments, like Fock states, squeezed states [3], superpositions of Fock states [4], and Schrödinger cat states [5]. Besides the fundamental aspect, the generation of entangled quantum states plays an important role in quantum computation, where a fundamental quantum logic gate has been realized experimentally [6]. In addition, various effective schemes for measuring the density matrix of the quantum motion of the trapped ion have been discovered. There are tomographical measurement schemes [7,8], QND schemes [9,10], quantum state endoscopy [11], and quantum reservoir engineering [12]. A possible method to measure entangled states of a trapped ion was proposed recently [13].

Although methods of creating special nonclassical states are already available [3–5], preparation of general quantum states remains an important challenge. This holds especially in the context of the generation of states in a truncated Hilbert space, like the well-known truncated Pegg-Barnett phase states [14], reciprocal-binomial states for determining the quantum optical phase [15], and truncated position eigenstates for constructing quantum states with maximal noise reduction [16], where the method of arbitrary state preparation is a required tool. Another application of arbitrary state preparation is the measurement of general motional observables [17].

In difference to the generation of special nonclassical states, an arbitrarily prescribed superposition of energy eigenstates requires a systematic production scheme. From the similarity between the Hamiltonians of the trapped ion system in the Lamb-Dicke limit and that of the Jaynes-Cummings model [18], a recent proposal of quantum state control in cavity QED [19] provided an obvious clue to the solution. The method was extended to the preparation of arbitrary motional states of a trapped ion beyond the Lamb-Dicke regime [17], where a nonlinear Jaynes-Cummings model applies [20]. In this paper, we shall describe several generalizations and extensions of the method in the trapped ion system. We direct our main attention to the production of the most general form of *entangled quantum states* whereby the ion's electronic (internal) degree of freedom and its external motion are quantum mechanically correlated in an arbitrary way.

In the case of the experimental generation of quantum states of a trapped ion, decoherence plays a crucial role, not only due to spontaneous emission but also due to technical errors like instabilities in laser and trap parameters [3]. For our scheme there is a need of many laser pulses. Therefore, we will examine the sensitivity of our method subjected to errors in controlling laser parameters, i.e., amplitude and phase.

In our method for preparing an arbitrary state, we start from the vacuum state of the ion's motion. A natural extension of this is the fundamental question: How can one evolve a system from a general initial state to a general target state? We will present a certain answer to this question in the form of a solution that works very efficiently for states that are localized in phase space.

Finally, we show how to entangle the internal state of the ion with two directions of the center-of-mass motion in an arbitrary way. This provides the possibility to prepare entangled quantum states in three degrees of freedom, i.e., generalized GHZ states [21]. We overcome the exponential dependence of the number of laser pulses to the upper phonon number, presented in a recent proposal of a two-dimensional (2D) scheme [17] for the center-of-mass motion of a trapped ion, by having a quadratic dependence in our scheme.

The organization of this paper is as follows. First, we describe the model and our scheme in Sec. II. Two examples that demonstrate quantum entanglement are given in Sec. III. In one of them we want to show perhaps one of the simplest ways of creating interesting quantum entanglement by separating the odd and even number states via entanglement with two electronic states. In Sec. IV, we present an analysis of the effects of technical noise on the target state. This analysis will be compared with numerical calculations, and the results can provide an error estimation with respect to realistic experimental parameters. Section V shows how to generate any state from any state. In Sec. VI we present our 2D scheme, and Sec. VII is devoted to our conclusions.

II. MODEL AND SCHEME

The quantized motion of the center of mass of a trapped ion is coupled to its electronic degree of freedom by external laser fields. In our model, we assume that the ion has effectively two electronic levels $|e\rangle$ and $|g\rangle$. The Hamiltonian of the system is given by [18]

$$\mathcal{H}(t)=\nu a^{\dagger}a+\tfrac{1}{2}E_0\sigma_z+(\lambda\sigma_{+}+\lambda^{*}\sigma_{-})\mathcal{E}(t) \tag{1}$$

(excluding a constant and setting $\hbar=1$), where ν is the vibration frequency of the ion in the harmonic potential, and $a^{\dagger}$ and a are the creation and annihilation operators associated with the ion's (harmonic) motion. The transition frequency between the two electronic levels is labeled by E_0, and the projection operators $\sigma_z=|e\rangle\langle e|-|g\rangle\langle g|$, $\sigma_{+}=|e\rangle\langle g|$ and $\sigma_{-}=|g\rangle\langle e|$ are given as in the usual Pauli matrix notation.

The dipole interactions between the ion and the laser fields are described by the last term of Eq. (1), where λ is the dipole coupling strength. In our scheme, the electric field $\mathcal{E}(t)$ is achieved by two running-wave lasers [22] propagating in the same direction x as the motion of the ion

$$\mathcal{E}(t)=\mathcal{E}^{c}(t)e^{i\eta_c(a+a^{\dagger})}e^{-i\omega_c t}+\mathcal{E}^{r}(t)e^{i\eta_r(a+a^{\dagger})}e^{-i\omega_r t}+\text{ H.c.} \tag{2}$$

Here we have expressed e^{ikx} explicitly in terms of the position operator $x=(a+a^{\dagger})/\sqrt{2\nu m}$ of the ion (where m is the mass of the ion). Therefore η_c and η_r are the so-called Lamb-Dicke parameters $\eta_i\equiv\omega_i/(c\sqrt{2m\nu})$ $(i=c,r)$. The frequencies of the lasers are chosen so that one laser is said to be tuned to the carrier frequency $\omega_c=E_0$, and the other one is said to be tuned to the red sideband $\omega_r=E_0-\nu$. Notice that the electric-field envelopes $\mathcal{E}^{c}(t)$ and $\mathcal{E}^{r}(t)$ are time dependent.

Transforming to an interaction picture by

$$|\Psi\rangle=e^{-i(\nu a^{\dagger}a+E_0\sigma_z/2)t}|\Psi\rangle_I, \tag{3}$$

the interaction Hamiltonian becomes

$$\mathcal{H}_{\text{int}}(t)=\lambda\{\mathcal{E}^{c}(t)e^{i\eta_c(ae^{-i\nu t}+a^{\dagger}e^{i\nu t})}\sigma_{+}+\mathcal{E}^{r}(t)e^{i\eta_r(ae^{-i\nu t}+a^{\dagger}e^{i\nu t})}e^{i\nu t}\sigma_{+}\}+\text{ H.c.}, \tag{4}$$

using a rotating-wave approximation. Since the vibration frequency ν is large compared with the Rabi frequency of the electronic transition [23], we can make further simplifications of Eq. (4) by keeping resonant interaction terms. This approximation was discussed in recent articles [18,20,24], and a nonlinear Jaynes-Cummings model can be derived. In our case the resonant terms describe the zero- and one-quantum transitions in the vibrational state of the ion going along with a transition in the internal state of the ion. We find that the Hamiltonian can be reduced to [25]

$$\mathcal{H}_{\text{int}}(t)=\sum_{n=0}^{\infty}c_n(t)|n\rangle\langle n|\sigma_{+}+\sum_{n=0}^{\infty}r_n(t)|n\rangle\langle n+1|\sigma_{+}+\text{ H.c.}, \tag{5}$$

where $c_n(t)$ and $r_n(t)$ are given by

$$c_n(t)=\lambda\mathcal{E}^{c}(t)e^{-\eta_c{}^2/2}L_n^0(\eta_c{}^2),$$

$$r_n(t)=\lambda\mathcal{E}^{r}(t)\frac{i\eta_r}{\sqrt{n+1}}e^{-\eta_r{}^2/2}L_n^1(\eta_r{}^2), \tag{6}$$

and $L_n^q(x)$ are the associated Laguerre polynomials [26].

Our aim is to prepare an arbitrary entangled state of the form

$$|\Psi_{\text{target}}\rangle=\alpha|\psi^{e},e\rangle+\beta|\psi^{g},g\rangle, \tag{7}$$

where

$$|\psi^{e}\rangle=\sum_{n=0}^{M}w_n^{e}|n\rangle,$$

$$|\psi^{g}\rangle=\sum_{n=0}^{M}w_n^{g}|n\rangle \tag{8}$$

are two normalized vibrational states associated with the excited and ground states, respectively, and α and β are weighting parameters that control the relative probability and phase between the ground and excited states. Since the probability amplitudes w_n^{e} and w_n^{g} are prescribed arbitrarily, the state $|\Psi_{\text{target}}\rangle$ represents the most general state in which the internal (electronic) states and the external (vibrational) states are entangled with each other. It should be remarked that the upper vibration quantum number M of our target state (7) can be any large integer that is only limited by the decoherence effects in experiments, in principle. We will assume that the time for generating our desired state is much shorter than the relaxation times due to spontaneous atomic decay and other damping effects, like the decoherence in the external atomic motion due to the use of an approximate Hamiltonian, which was discussed in Ref. [17], or due to technical errors. In Sec. IV, we look at the effects of fluctuations in the external fields as a certain damping effect, that has not been discussed in literature but is very important for arbitrary state preparation.

The strategy for creating target state (7) is based on the unitary time evolution generated by Hamiltonian (5). We choose the initial state to be the ground state of the system $|\Psi_{\text{initial}}\rangle=|0,g\rangle$, that is already achievable in recent laser cooling [23], and state preparation experiments [3–5]. Our goal is to conduct the evolution of the system from this initial state to the target state (7) at time T,

$$|\Psi_{\text{target}}\rangle=\mathcal{U}(T,0)|\Psi_{\text{initial}}\rangle, \tag{9}$$

where $\mathcal{U}(T,0)$ is the time-evolution operator.

In our preparation scheme $\mathcal{U}(T,0)$ is realized by switching the lasers on the carrier and red sideband on and off, alter-

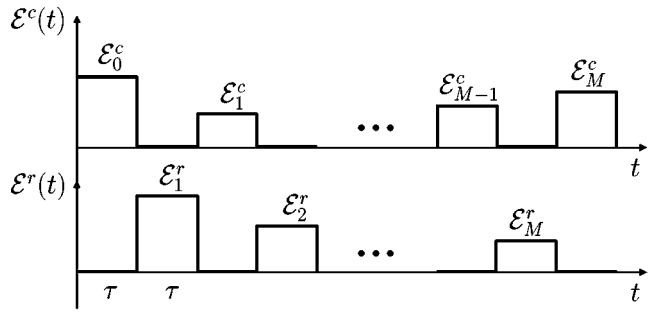

FIG. 1. Our preparation scheme is designed by switching the lasers on the carrier and red sideband, on and off alternately.

nately, according to Fig. 1. We divide the time interval $[0,T]$ into $(2M+1)$ subintervals which have all the same length $\tau=T/(2M+1)$, for simplicity. During each time subinterval, we turn the laser fields on and off as

$$\mathcal{E}^c(t)=\mathcal{E}_j^c, \quad \mathcal{E}^r(t)=0 \tag{10}$$

for $t\in[2j\tau,(2j+1)\tau)$ and $j=0,\ldots,M$;

$$\mathcal{E}^c(t)=0, \quad \mathcal{E}^r(t)=\mathcal{E}_j^r \tag{11}$$

for $t\in[(2j-1)\tau,2j\tau)$ and $j=1,\ldots,M$; where $\{\mathcal{E}_j^{c,r}\}$ is a set of to be determined electric fields with constant amplitude and phase for $j=(0),1,\ldots,M$.

With these definitions of the fields, the evolution operator $\mathcal{U}(T,0)$ can be written as a sequence of unitary operators [27] associated with the time subintervals

$$\begin{aligned}\mathcal{U}(T,0)&=\mathcal{U}(2M+1)\cdot\mathcal{U}(2M)\cdots\mathcal{U}(2j+1)\\&\quad\cdot\mathcal{U}(2j)\cdots\mathcal{U}(3)\cdot\mathcal{U}(2)\cdot\mathcal{U}(1)\\&=C_M\cdot R_M\cdots C_j\cdot R_j\cdots C_1\cdot R_1\cdot C_0,\end{aligned} \tag{12}$$

where $\mathcal{U}(k)\equiv\mathcal{U}(k\tau,(k-1)\tau)$ for $k=1,\ldots,2M+1$. For our convenience, we used C_j and R_j for the evolution due to the laser at the carrier frequency and red sideband, respectively. In the basis

$$|n,e\rangle\equiv\begin{pmatrix}1\\0\end{pmatrix}, \quad |n,g\rangle\equiv\begin{pmatrix}0\\1\end{pmatrix} \tag{13}$$

for $n=0,\ldots,M$; C_j can be expressed as 2×2 matrices C_j^n,

$$C_j^n=\begin{pmatrix}\cos|c_{n,j}|\tau & -i\,e^{i\theta_j^c}\sin|c_{n,j}|\tau\\ -i\,e^{-i\theta_j^c}\sin|c_{n,j}|\tau & \cos|c_{n,j}|\tau\end{pmatrix}, \tag{14}$$

for $j=0,\ldots,M$. In the basis

$$|n-1,e\rangle\equiv\begin{pmatrix}1\\0\end{pmatrix}, \quad |n,g\rangle\equiv\begin{pmatrix}0\\1\end{pmatrix} \tag{15}$$

for $n=1,\ldots,M$; R_j can be expressed as 2×2 matrices R_j^n,

$$R_j^n=\begin{pmatrix}\cos|r_{n-1,j}|\tau & -i\,e^{i\theta_j^r}\sin|r_{n-1,j}|\tau\\ -i\,e^{-i\theta_j^r}\sin|r_{n-1,j}|\tau & \cos|r_{n-1,j}|\tau\end{pmatrix}, \tag{16}$$

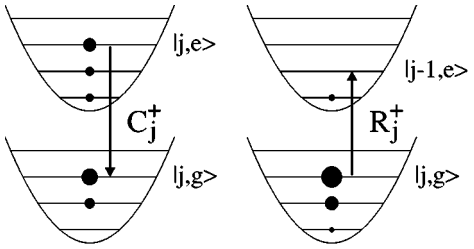

FIG. 2. Here the transitions involved with one sequence of two pulses $C_j^\dagger$ and $Q_j^\dagger$ are shown. We plotted the energy-level scheme for our system without scaling. The occupation probabilities $|w_n^a|^2$, $a=g,e$, are represented by circles. On the left side $C_j^\dagger$ ''sweeps'' down the probability from the level $|j,e\rangle$ to $|j,g\rangle$. On the right side we see the state with the changed probabilities after this pulse. There we also show the effect of $R_j^\dagger$ that brings ''down'' the probability from $|j,g\rangle$ to $|j-1,e\rangle$.

for $j=1,\ldots,M$. The state $|0,g\rangle$ is a dark state, i.e., it is not coupled to any other state, when the laser is tuned to the red sideband. In the previous equations we defined $c_{n,j}=|c_{n,j}|\exp(i\theta_j^c)$ and $r_{n,j}=|r_{n,j}|\exp(i\theta_j^r)$. We decomposed the problem into complex rotations between two levels.

We determine the moduli and phases of the electric fields $\{\mathcal{E}_j^{c,r}\}$ by inverting the unitary time evolution (12)

$$|0,g\rangle=\mathcal{U}(0,T)|\Psi_{\text{target}}\rangle=C_0^\dagger R_1^\dagger C_1^\dagger\cdots R_M^\dagger C_M^\dagger|\Psi_{\text{target}}\rangle. \tag{17}$$

This equation can be solved for *every* $|\Psi_{\text{target}}\rangle$ as given in Eq. (7), because the sequence of operators on the right-hand side of Eq. (17) can transfer all the probability in higher-energy levels of our target state to the energy ground state $|\Psi_{\text{initial}}\rangle=|0,g\rangle$, step by step (see Fig. 2) on our constructed stairway (see Fig. 3). That means that we fulfill the conditions

$$\langle j,e|C_j^\dagger|F_{j+1}\rangle=0 \qquad \text{for } j=0,\ldots,M, \tag{18}$$

$$\langle j,g|R_j^\dagger C_j^\dagger|F_{j+1}\rangle=0 \qquad \text{for } j=1,\ldots,M, \tag{19}$$

where

$$|F_{j+1}\rangle\equiv R_{j+1}^\dagger C_{j+1}^\dagger\cdots R_M^\dagger C_M^\dagger|\Psi_{\text{target}}\rangle \tag{20}$$

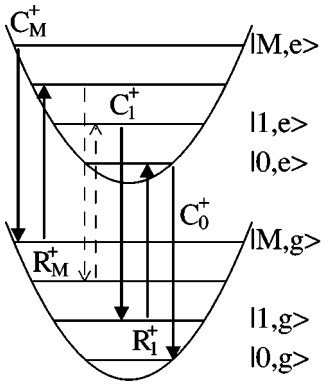

FIG. 3. With the arranged sequence of unitary operators in Eq. (12) we find a way to bring down all the probability from every target state to the initial state.

for $j=0,\ldots,M-1$ and $|F_{M+1}\rangle\equiv|\Psi_{\text{target}}\rangle$. The condition relations (18) and (19) provide the following equations to determine the set of Rabi frequencies $\{c_j;j=0,\ldots,M\}$, $\{r_j;j=1,\ldots,M\}$:

$$\tan|c_j|\tau=\frac{i\alpha_j\, e^{-i\theta_j^c}}{\beta_j} \tag{21}$$

for $j=0,\ldots,M$, and

$$\tan|r_j|\tau=\frac{i\mu_j\, e^{i\theta_j^r}}{\gamma_j} \tag{22}$$

for $j=1,\ldots,M$, where we used

$$\alpha_j=\langle j,e|F_{j+1}\rangle, \tag{23}$$

$$\beta_j=\langle j,g|F_{j+1}\rangle, \tag{24}$$

$$\mu_j=\langle j,g|C_j^\dagger|F_{j+1}\rangle, \tag{25}$$

$$\gamma_j=\langle j-1,e|C_j^\dagger|F_{j+1}\rangle, \tag{26}$$

and the new definitions $c_{j,j}\equiv c_j$ and $r_{j-1,j}\equiv r_j$. With the set of Rabi frequencies received from Eqs. (21) and (22), we determine the set of electric fields $\{\mathcal{E}_j^{c,r};j=(0),1,\ldots,M\}$ by inverting Eq. (6) in the following way [28]:

$$\mathcal{E}_j^c=c_j\frac{e^{\eta_c{}^2/2}}{L_j^0(\eta_c{}^2)\lambda}\qquad\text{for } j=0,\ldots,M, \tag{27}$$

$$\mathcal{E}_j^r=r_j\frac{e^{\eta_r{}^2/2}\sqrt{j}}{L_{j-1}^1(\eta_r{}^2)\lambda\, i\,\eta_r}\qquad\text{for } j=1,\ldots,M. \tag{28}$$

Since a solution for Eqs. (21) and (22) always exists [29], we can indeed prepare any arbitrary entangled target state $|\Psi_{\text{target}}\rangle$ in the time T.

III. EXAMPLES

A. Example: ''clock'' state

In this section we will give an example for the generation of an arbitrary entangled state. For this we invent a ''clock'' state

$$|\text{clock}\rangle=|\Theta_{k_h}^h\rangle|g\rangle+|\Theta_{k_m}^m\rangle|e\rangle, \tag{29}$$

where $|\Theta_{k_h}^h\rangle$ and $|\Theta_{k_m}^m\rangle$ are truncated Pegg-Barnett phase states [14],

$$|\Theta_{k_h}^h\rangle=\frac{1}{\sqrt{M_h+1}}\sum_{n=0}^{M_h}e^{in\Theta_{k_h}^h}|n\rangle, \tag{30}$$

$$|\Theta_{k_m}^m\rangle=\frac{1}{\sqrt{M_m+1}}\sum_{n=0}^{M_m}e^{in\Theta_{k_m}^m}|n\rangle, \tag{31}$$

with the phase angles defined by

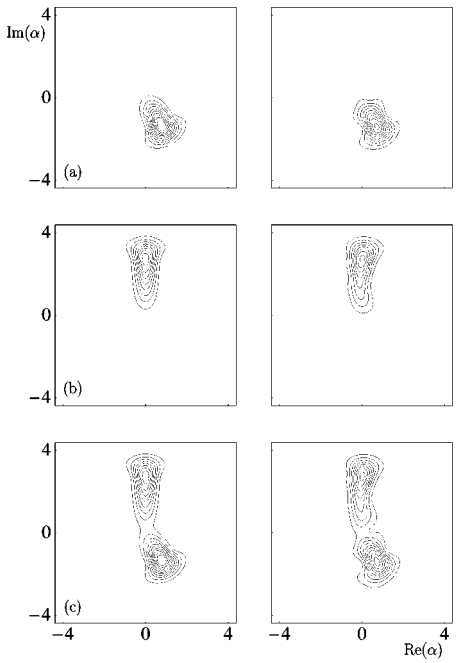

FIG. 4. Contour plots for the Q functions (a) $|\langle\alpha,g|\text{clock}\rangle|^2$ and (b) $|\langle\alpha,e|\text{clock}\rangle|^2$. In each of the two Q functions, information about the center-of-mass motion of the ion is partly included. (c) Contour plot for the Q function of the external motion of the clock state when the atomic variables are traced out. The full time information is exhibited here. Left column: unperturbed preparation; right column: wrong parameters for laser amplitudes and phases. The inner circle is at 0.13 for all Q-function plots.

$$\Theta_{k_h}^h=\frac{\pi}{2}-\frac{2\pi k_h}{M_h+1}\qquad\text{and}\quad k_h=1,\ldots,M_h+1,$$

$$\Theta_{k_m}^m=\frac{\pi}{2}-\frac{2\pi k_m}{M_m+1}\qquad\text{and}\quad k_m=1,\ldots,M_m+1. \tag{32}$$

It is known that truncated Pegg-Barnett phase states have well-localized phase angles. Hence, the Q function of the clock state (see the left column of Fig. 4) exhibits two arms located at angles $\Theta_{k_h}^h$ and $\Theta_{k_m}^m$. We may view $|\Theta_{k_h}^h\rangle$ as the hand for the hours of a clock, and $|\Theta_{k_m}^m\rangle$ as the hand for the minutes. Because the two phase states are truncated at different upper phonon numbers M_h and M_m, the phase intervals $\Delta\Theta^h=2\pi/(M_h+1)$ and $\Delta\Theta^m=2\pi/(M_m+1)$ are different. In this example, we choose $M_h=11$ and $M_m=29$ so that the hand for the minutes is long and thin, and the hand for the hours is small and thick. For our convenience we have chosen $M_m=29$ and not $M_m=59$, as it would be necessary for a real clock. Therefore the time of our clock is only ''exact'' in the range of two minutes. In the left part of Fig. 4 we present contour plots of the Q function,

$$Q_h(\alpha)=|\langle\alpha,g|\text{clock}\rangle|^2=|\langle\alpha|\Theta_{k_h}^h\rangle|^2, \tag{33}$$

$$Q_m(\alpha)=|\langle\alpha,e|\text{clock}\rangle|^2=|\langle\alpha|\Theta_{k_m}^m\rangle|^2, \tag{34}$$

for the hour and minute hands, respectively, when we project the clock state onto corresponding atomic states. The overall

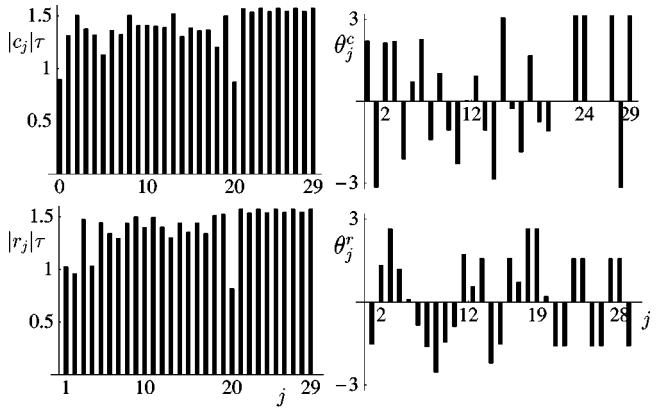

FIG. 5. Diagrams for the amplitudes $|r_j|\tau$ and $|c_j|\tau$, and the phases θ_j^r and θ_j^c of the lasers required to generate the clock state. They are labeled by j, that is, the number of the pulses according to Eq. (12).

look of the clock is obtained by tracing out the atomic variables, and the Q function of the reduced density matrix is given by

$$Q_{tr}(\alpha)=Q_h(\alpha)+Q_m(\alpha); \tag{35}$$

see Fig. 4(c). For our numerical example in Fig. 4 we set $k_h=5$ and $k_m=0$ to set our clock to 5 o'clock.

The numerical values of amplitudes and phases for the required laser pulses are displayed in Fig. 5. In the left part of Fig. 5 the upper plot shows $|r_j|\tau$ for the red sideband laser, and the lower plot shows $|c_j|\tau$ for the laser on the carrier frequency. In the right part of Fig. 5 the upper plot shows the values for the phases θ_j^r for the red sideband laser, and the lower plot shows the phases θ_j^c for the laser on resonance. These amplitudes and phases look rather complicated, which should be expected because of the complexity of our chosen state.

B. Separation of odd and even number states

We will show perhaps one of the simplest ways of creating interesting quantum entanglement, where the odd and even-number states are separated by entanglement with the two atomic states. If we choose always to do π pulses [30] of the resonant laser, so that $c_n\tau=\pi/2$ [31] and the number M is odd (even), then the ground atomic state entangles only to even (odd) number vibrational states, and the excited atomic state entangles only to odd (even) number vibrational states; i.e., for M odd the target state is

$$|\Psi_{\text{target}}\rangle=\sum_{n=0}^{(M-1)/2} w_{2n}^g|2n,g\rangle+\sum_{n=0}^{(M-1)/2} w_{2n+1}^e|2n+1,e\rangle. \tag{36}$$

In other words, the odd and even number states are separated via entanglement. This is a general result that does not depend on parameters in the red sideband channel.

One can understand this by defining the two manifolds $\{|2n,g\rangle,|2n+1,e\rangle\}$ and $\{|2n+1,g\rangle,|2n,e\rangle\}$. R_j invokes only transitions within the manifolds, and in case of a π pulse C_j interchanges occupations between the manifolds completely. Starting with an intermediate state

$$|\psi_{\text{im}}\rangle=\sum_n a_n|2n,g\rangle+\sum_n b_n|2n+1,e\rangle, \tag{37}$$

the sequence C_jR_j shifts the occupations into the other manifold:

$$C_jR_j|\psi_{\text{im}}\rangle=\sum_n c_n|2n+1,g\rangle+\sum_n d_n|2n,e\rangle. \tag{38}$$

Another sequence $C_{j+1}R_{j+1}$ will shift the occupations into the first manifold again. Note that this works because of the initial condition $C_0|0,g\rangle=|0,e\rangle$, i.e., we start from one of the two manifolds.

IV. ERROR ANALYSIS

In this section we examine the robustness of our scheme on errors occuring in laser parameters. The laser parameters relevant to our scheme are the amplitudes and phases of the fields

$$\mathcal{E}_j^\alpha\equiv|\mathcal{E}_j^\alpha|e^{i\theta_j^\alpha}. \tag{39}$$

The subscript $j=(0),1,\ldots,M$ and the superscript $\alpha=r,c$ label the interactions corresponding to R_j or C_j. We denote the errors

$$\delta|\mathcal{E}_j^\alpha|=|\mathcal{E}_j^\alpha|-|\overline{\mathcal{E}_j^\alpha}|, \tag{40}$$

$$\delta\theta_j^\alpha=\theta_j^\alpha-\overline{\theta_j^\alpha}, \tag{41}$$

with $\overline{\mathcal{E}_j^\alpha}$ and $\overline{\theta_j^\alpha}$ representing the parameters for the generation of the target state. Hence, for each set of the electric fields, a final state $|\Psi_f\rangle$

$$|\Psi_f\rangle=\mathcal{U}(T,0;\{\mathcal{E}_j^\alpha\})|\Psi_{\text{initial}}\rangle \tag{42}$$

is generated. We want to determine the difference between the final state and the target state. This is measured by the overlap

$$P\equiv|\langle\Psi_{\text{target}}|\Psi_f\rangle|^2, \tag{43}$$

so that $P=1$ indicates the perfect situation in which the target state is obtained (up to an overall phase factor).

Because of the random nature of the errors, a useful description of their influence is the average value of P with respect to many experimental trials,

$$\overline{P}=\frac{1}{N}\sum_{i=1}^N P_i, \tag{44}$$

where N is the number of trials. For simplicity, we make the natural assumption that the errors in Eqs. (40) and (41) are mutually independent, and that their means are zero. In other words, the errors for any two different laser pulses are not correlated.

We are only interested in the small perturbation regime where $\delta|\mathcal{E}_j^\alpha|\ll|\overline{\mathcal{E}_j^\alpha}|$ and $\delta\theta_j^\alpha\ll\overline{\theta_j^\alpha}$. In this case, we can expand the time evolution operators to the second order of the errors. With the help of the statistical independence assumption, we can estimate that

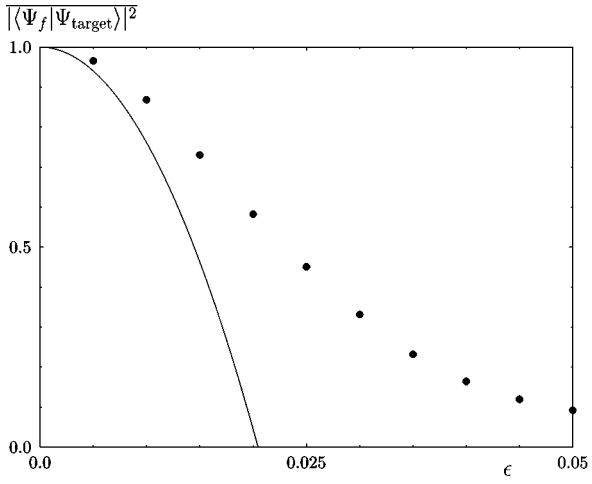

FIG. 6. Effect on the prepared state by a Gaussian error ϵ in all laser parameters according to Eqs. (46) and (47). The circles are the numerically calculated values for the averaged overlap of an exact target state and a wrongly prepared clock state. The solid line is the theoretically estimated lower bound of Eq. (45).

$$\overline{P} \geqslant 1 - \sum_{j=0}^{M} [\lambda^2 \overline{(\delta|\mathcal{E}_j^c|)^2} + \overline{(\delta\theta_j^c)^2}] - \sum_{j=1}^{M} [j\lambda^2 \eta_r^2 \overline{(\delta|\mathcal{E}_j^r|)^2} + \overline{(\delta\theta_j^r)^2}]. \quad (45)$$

This inequality provides a statistical measure of the robustness of our scheme in the small error limit. We see that the smallest value of $\overline{P}$ is always bounded according to Eq. (45).

We tested our analytical result numerically by generating wave functions with an error in all laser parameters. The error in the laser amplitudes, what is actually an error in the pulse area, can be seen to be fractional:

$$\frac{\overline{(\delta|\mathcal{E}_j^c|)^2}^{1/2}}{|\mathcal{E}_j^c|} = \frac{\overline{(\delta|\mathcal{E}_j^r|)^2}^{1/2}}{|\mathcal{E}_j^r|} = \epsilon_a . \quad (46)$$

The error in the phase of the laser should be absolute. But we weight it by the maximal value 2π of the phase to have a comparison with the relative error in the amplitude

$$\frac{\overline{(\delta\theta_j^c)^2}^{1/2}}{2\pi} = \frac{\overline{(\delta\theta_j^r)^2}^{1/2}}{2\pi} = \epsilon_p . \quad (47)$$

The errors had always a Gaussian distribution with zero mean and standard deviations ϵ_a or ϵ_p, respectively. We tested the creation of the clock state for $M=29$, described in Sec. III. Our numerical and analytical results are shown in Fig. 6. There the number of calculated wave functions for obtaining the average of the overlap $\overline{P}$ is $N=1000$. We defined the standard deviations $\epsilon_a=\epsilon_p=\epsilon$ to have a comparable amplitude and phase error. The chosen Lamb-Dicke parameter is $\eta_r=0.1$. The circles are the numerically calculated values for the averaged overlap of exact target state and wrongly prepared clock state. The solid line is the theoretically estimated lower bound of Eq. (45). We see a good agreement of our estimation (45), that is excellent for small ϵ, which is expected as our analytical estimation is for the small error regime. We see that for the error parameter $\epsilon=0.01$ the overlap of the created state and our target state is 0.87 and so our state preparation scheme still works quite well.

In the right column of Fig. 4, we calculate only one random final wave function. For this example we chose $\epsilon=0.01$ and a very nice representative of the Q function. On the right–hand side of Figs. 4(a) and 4(b), we present the contour plots for the Q functions $|\langle\alpha,g|\Psi_f\rangle|^2$ and $|\langle\alpha,e|\Psi_f\rangle|^2$ of the external motion of the wrongly prepared clock state, when this one is projected onto the atomic ground or excited state. The probability that the atom is in the ground state is 0.48 in this one run, and 0.52 that it is in the excited state. In the right part of Fig. 4(c) we show the contour plot for the Q function of the external motion of the wrongly prepared clock state, when we trace out the atomic variables. In this example the overlap with the correct target state is 0.85, whereas the average from Fig. 6 is 0.87. Thus it represents a good example of the usual outcome of the experiment. We still can recognize that it is 5 o'clock. This effect and the shape of our clock reminds us of ''the persistence of memory'' that our state preparation scheme has.

V. CONTROL OF THE TIME EVOLUTION OF A QUANTUM STATE

Is it possible to evolve a system from a general initial state to a general target state,

$$|\psi(t)\rangle = U(t,t')|\psi(t')\rangle, \quad (48)$$

so that one can control the unitary time evolution of a quantum system completely? One can imagine that there is a fundamental limit concerning the time difference $\Delta t=t-t'$, that is to say the switching time, for every quantum system. In our case this limit is given by neglecting the nonresonant terms in the order of the ion's vibration frequency ν in the interaction Hamiltonian (4); therefore we have to accept $\Delta t \gg 1/\nu$ [24]. In this section we concentrate only on the preparation of motional quantum states.

With the help of Sec. II, we can see easily that it is possible to generate a general state from another general state by going over the system's ground state $|0,g\rangle$. This is not a very efficient method for most states. Therefore we propose a modified preparation scheme, that works very efficiently for states localized in phase space by preparing over a coherent state as an intermediate state. For this, we show how to prepare an arbitrary state out of a coherent state $|\alpha\rangle$. We can use the same laser configuration as in Sec. II, but we require a phase modulation of the lasers. For the laser on resonance we have to replace $\mathcal{E}^c(t)$ by $\mathcal{E}^c(t)\ \exp[-i\eta_c\ \mathrm{Re}(\alpha\, e^{-i\nu t})]$, and for the detuned laser we have to replace $\mathcal{E}^r(t)$ by $\mathcal{E}^r(t)\ \exp[-i\eta_r\ \mathrm{Re}(\alpha\, e^{-i\nu t})]$ in our interaction Hamiltonian (4). With this phase modulation we work in a phase space displaced by α. Therefore the coherent state $|\alpha\rangle$ plays the role of the vacuum state, and displaced Fock states play the role of the Fock states in the undisplaced Hilbert space, respectively. Therefore we can use the same method of Sec. II for determining the amplitudes $\mathcal{E}^c(t)$ and $\mathcal{E}^r(t)$; we just have to transform our target state to the displaced frame [32].

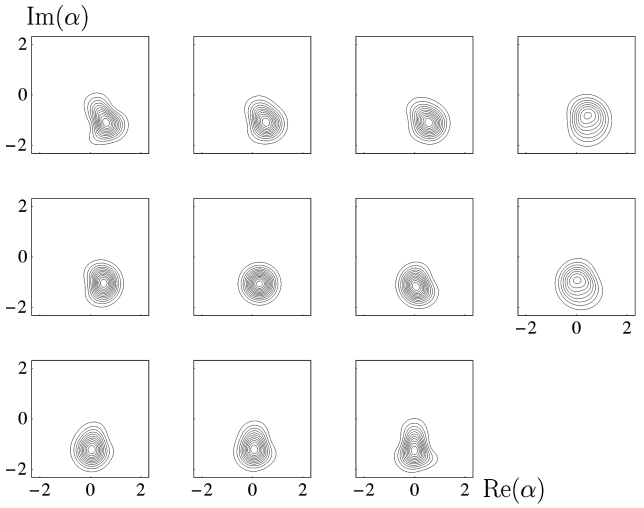

FIG. 7. Illustration of a state preparation scheme with an arbitrary initial state: The hour hand moves from 5 to 6. Snapshots of the time evolution of the Q function are shown after each RC pulse by tracing out the internal variables.

Thus we can prepare any state from any state by the sequence

$$|\psi_{\text{target}},g\rangle=\widetilde{R}_{f,1}\cdots\widetilde{R}_{f,j}\cdot\widetilde{C}_{f,j}\cdots\widetilde{C}_{f,M}\cdot\widetilde{C}^{\dagger}_{t,M}\cdots\widetilde{C}^{\dagger}_{t,j}\cdot\widetilde{R}^{\dagger}_{t,j}\cdots\widetilde{R}^{\dagger}_{t,1}|\psi_{\text{initial}},g\rangle, \tag{49}$$

where the target state $|\psi_{\text{target}}\rangle$ and the initial state $|\psi_{\text{initial}}\rangle$ are general states in the displaced Fock state basis, and where $\widetilde{C}^{\dagger}_{t,j}$ and $\widetilde{R}^{\dagger}_{t,j}$ are unitary evolutions due to the new interaction Hamiltonian with the phase-modulated lasers from the initial state $|\psi_{\text{initial}}\rangle$ backwards to a coherent state $|\alpha\rangle$

$$|\alpha,g\rangle=\widetilde{C}^{\dagger}_{t,M}\cdots\widetilde{C}^{\dagger}_{t,j}\cdot\widetilde{R}^{\dagger}_{t,j}\cdots\widetilde{R}^{\dagger}_{t,1}|\psi_{\text{initial}},g\rangle, \tag{50}$$

and $\widetilde{R}_{f,j}$ and $\widetilde{C}_{f,j}$ lead from $|\alpha\rangle$ in a unitary evolution to the target state $|\psi_{\text{target}}\rangle$,

$$|\psi_{\text{target}},g\rangle=\widetilde{R}_{f,1}\cdots\widetilde{R}_{f,j}\cdot\widetilde{C}_{f,j}\cdots\widetilde{C}_{f,M}|\alpha,g\rangle. \tag{51}$$

As we discussed, the amplitudes $\mathcal{E}^{c}_{t,j}$, $\mathcal{E}^{r}_{t,j}$, $\mathcal{E}^{c}_{f,j}$, and $\mathcal{E}^{r}_{f,j}$ are determined as in Sec. II. The amplitude of the coherent state α is defined best by lying between the two localized states $|\psi_{\text{target}}\rangle$ and $|\psi_{\text{initial}}\rangle$, i.e.,

$$\alpha=\tfrac{1}{2}(\langle\psi_{\text{initial}}|\hat{a}|\psi_{\text{initial}}\rangle+\langle\psi_{\text{target}}|\hat{a}|\psi_{\text{target}}\rangle). \tag{52}$$

In our example (Fig. 7), we show snapshots of the unitary evolution for moving the hour hand from 5 o'clock to 6 o'clock. With this new preparation scheme, by preparing over a coherent state only 20 pulses are needed, instead of 44 when preparing over the vacuum state. Thus it works very efficiently.

In the Lamb-Dicke regime there is another possible way to prepare any state from any state. Instead of the phase-modulated lasers, we can switch on the laser on resonance all the time, see Fig. 8. When the red detuned laser is switched

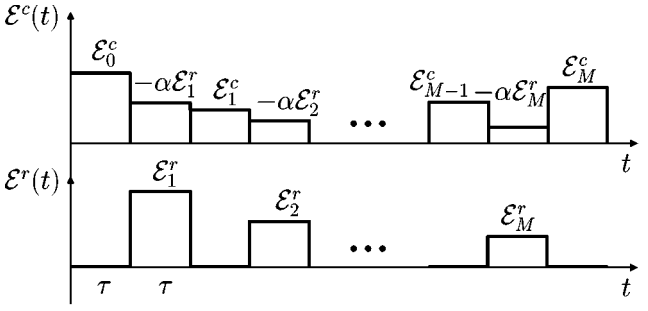

FIG. 8. A preparation scheme for generating a general target state starting from a general initial state in the Lamb-Dicke regime.

on with amplitude $\mathcal{E}^{r}_{j}$, we also switch on the laser on resonance with amplitude $-\alpha\mathcal{E}^{r}_{j}$. Doing this, we work in a phase space displaced by α.

VI. 2D SCHEME

The general quantum state of our system, if we include two motional degrees of freedom, i.e., the x and y directions, has the form of Eq. (7), but with

$$|\psi^{e}\rangle=\sum_{n_x=0}^{M_x}\sum_{n_y=0}^{M_y}\xi^{e}_{n_x n_y}|n_x,n_y\rangle,$$

$$|\psi^{g}\rangle=\sum_{n_x=0}^{M_x}\sum_{n_y=0}^{M_y}\xi^{g}_{n_x n_y}|n_x,n_y\rangle, \tag{53}$$

where $|\psi^{e,g}\rangle$ are general 2D harmonic-oscillator states, with M_x and M_y being the highest phonon number in directions x and y, respectively. Being able to synthesize such a state, one is able to generate generalized GHZ states [21],

$$|\Psi\rangle=\frac{1}{\sqrt{2}}(|0_x,0_y,g\rangle+|M_x,M_y,e\rangle). \tag{54}$$

The simplest way of extending the arbitrary state preparation method to two dimensions is to use the same ideas of inverting the unitary time evolution and of ''sweeping down'' the probability. Here one might first clear one dimension by ''sweeping down'' the probability column by column, and collect the probability in the second dimension in the last step, according to Fig. 9. Described by an unitary time evolution, the preparation scheme reads

$$|\Psi_{\text{target}}\rangle=\left(\prod_{j=0}^{M_y}C_{M_x,j}R_{M_x,j}\cdots C_{1,j}R_{1,j}C_{0,j}\right)\times R_{M_y}C_{M_y-1}R_{M_y-1}\cdots C_1R_1C_0|0_x,0_y,g\rangle. \tag{55}$$

However, there is the problem of a leak-out of probability, since, if one clears one column, there are resonant interactions in the other columns, and the probability ''climbs up the ladder,'' in general, in contrast to the intention. However, there is still a way to catch the escaping probability, as demonstrated nicely in Ref. [17]. But the price one pays for this

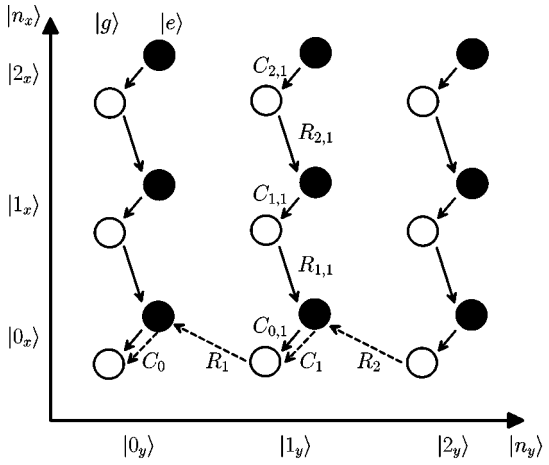

FIG. 9. The 2D scheme. Column by column from right to left is projected down with the 1D method in combination with a dynamical Stark-effect-like interaction that provides a large detuning for the columns not considered. Finally, row $|0_x\rangle$ is projected onto the initial state $|0_x,0_y,g\rangle$ (dashed arrows).

is the exponential dependence of the number of laser pulses on the upper phonon numbers M_x and M_y.

For the first proposed way, the number of pulses is $(M_y+1)(2M_x+1)+2M_y$, that is, proportional to M_xM_y. Hence one has to find another way that prevents the leak-out of probability. The central idea of how to do this is to introduce an interaction that keeps the column on resonance, which we do in 1D state preparation, and to keep all other columns off resonance. This means that one needs a phonon-number-dependent interaction for one direction, i.e., the y direction,

$$H_{\rm int}^{\rm 2D}=f(a_y^\dagger a_y)\sigma_z, \tag{56}$$

which is a kind of dynamical Stark effect. The details of this scheme for the cavity QED case are described elsewhere [33]. Here we want to discuss the implementation of this interaction Hamiltonian to the Paul trap. The 2D Hamiltonian is given by

$$\mathcal{H}(t)=\nu_x a_x^\dagger a_x+\nu_y a_y^\dagger a_y+\tfrac{1}{2}E_0\sigma_z+(\vec{\lambda}\sigma_+ +\vec{\lambda}^*\sigma_-)\vec{\mathcal{E}}(t). \tag{57}$$

The electric field consists of the field (2) in the x direction for the 1D state preparation and a standing-wave laser field $\mathcal{E}_y(t)=\mathcal{E}_s\cos(k_s\hat{y})\cos(\omega_s t)$ in the y direction with detuning $\Delta_y=\omega_s-\omega_0$. Defining the frequencies $\omega_c=E_0+\Delta_x$ and $\omega_r=E_0-\nu+\Delta_x$, we choose a variable detuning Δ_x of the lasers in the x direction. With the two usual rotating-wave approximations and for large detuning $|\Delta_y|\gg|\lambda_y\mathcal{E}_s|$ of the standing wave, this yields the Hamiltonian

$$\mathcal{H}_{\rm int}(t)=\mathcal{H}_{\rm int}^{\rm 1D}(t)-\tfrac{1}{2}\sum_{n_y=0}^{\infty}(\Delta_x+s_{n_y})|n_y\rangle\langle n_y|\sigma_z \tag{58}$$

in an interaction picture with the transformation $\exp[-i(\nu_x a_x^\dagger a_x+\nu_y a_y^\dagger a_y+(E_0+\Delta_x)\sigma_z/2)t]$, where $\mathcal{H}_{\rm int}^{\rm 1D}(t)$ is the 1D interaction Hamiltonian (5), and

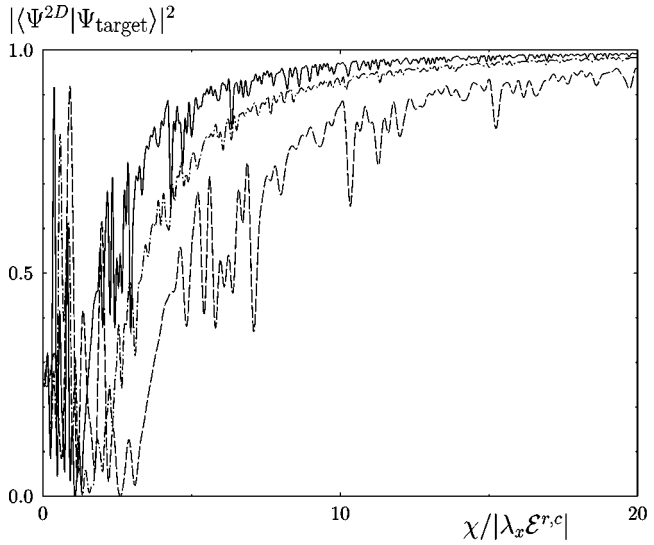

FIG. 10. Overlap between the 2D target state and the prepared state, using the full Hamiltonian. We see the convergence to 1 for increasing $\chi/|\lambda_x\mathcal{E}^{r,c}|$. Lamb-Dicke parameters: $(\eta_s,\eta_{r,c})=(0.4,0.2)$ (full line), (0.4,0.5) (dash-dotted line), and (0.2,0.2) (dashed line).

$$s_{n_y}=\frac{|\lambda_y\mathcal{E}_s|^2}{\Delta_y}\{1+e^{-(2\eta_s)^2/2}L_{n_y}^0((2\eta_s)^2)\}. \tag{59}$$

By setting $\Delta_x(n_y)=-s_{n_y}$, we can address a certain column $|n_y\rangle$, that is then on resonance and other columns $|n_y'\rangle$ that are off resonance with the detuning $\delta=s_{n_y'}-s_{n_y}\propto|\lambda_y\mathcal{E}_s|^2/\Delta_y$. If this detuning is large enough compared to the Rabi frequencies (6) of the 1D state preparation method, then our 2D scheme will work.

We illustrate this in Fig. 10 by preparing state (54) for $M_x=M_y=3$. As a measure of the successful preparation of the state, we use the overlap between target state $|\Psi_{\rm target}\rangle$ and the state $|\Psi^{\rm 2D}\rangle$ prepared by our Hamiltonian (58). We see that for increasing $\chi=|\lambda_y\mathcal{E}_s|^2/\Delta_y$ the overlap converges to 1. Here χ is scaled in $|\lambda_x\mathcal{E}^{r,c}|$, where $\mathcal{E}^{r,c}$ are chosen to be constant and the time τ_j for every pulse is variable, as argued in Ref. [28]. Further the overlap depends on the Lamb-Dicke parameters η_s and $\eta_{r,c}$. In Fig. 10 we observe that the scheme works best for small parameters $\eta_{r,c}$, as the Rabi frequencies (6) have their maxima in the Lamb-Dicke limit. The dependence of the overlap on η_s is not that trivial, because one has to optimize to the maximal $|\delta|$'s for all n_y and n_y'. Therefore the best chosen η_s depends highly on the target state. In our case this was $\eta_s=0.4$.

In general, one can find always a combination of η_s and $\eta_{r,c}$, so that the target state is prepared better than 90% for $\chi/|\lambda_x\mathcal{E}^{r,c}|\approx 10$. This value can be achieved experimentally by a very good fulfillment of the strong-coupling regime. The generalization to a 3D scheme is straightforward by the introduction of a standing-wave laser in the z direction.

VII. CONCLUDING REMARKS

In conclusion, we have presented a systematic method to prepare general quantum states of a trapped ion where quantum entanglement between the center-of-mass motion and

the electronic state can be manipulated arbitrarily. Further, we have shown a very simple way to generate interesting quantum entanglement by separating odd and even number states via the two atomic states. We have estimated errors due to technical noise in pulse areas and phases of the lasers. This kind of error becomes important, because of the need of many laser pulses.

We have described a method to generate a general target state starting from a general initial state, which is a worthwhile extension of the arbitrary state preparation method, that so far has been restricted to an initial vacuum state. This opens the possibility of full control of the quantum system's time evolution, i.e., the ion's quantum-mechanical center-of-mass motion.

We have presented a preparation scheme for arbitrary entangled quantum states in three degrees of freedom, consisting of two degrees for the center-of-mass motion of the trapped ion and of one degree for its internal electronic structure. We point out that an experimental realization of the 1D scheme seems to be achievable with the current kind of experiments [3–5], but high control of pulse areas and phases of the lasers is needed.

ACKNOWLEDGMENTS

We thank J. H. Eberly, W. Vogel, D. J. Wineland, D. M. Meekhof, M. Kalinski, and M. Freyberger for valuable conversations. B.K. gratefully acknowledges the hospitality of the NSF Rochester Theory Center for Optical Science and Engineering at the University of Rochester, and gratefully acknowledges support from the Deutsche Forschungsgemeinschaft. This work was supported in part by the National Science Foundation under Grant No. PHY 94-15583.

[1] E. Schrödinger, Naturwissenschaften **23**, 807 (1935).
[2] A. Einstein, B. Podolsky, and N. Rosen, Phys. Rev. **47**, 777 (1935).
[3] D. M. Meekhof, C. Monroe, B. E. King, W. M. Itano, and D. J. Wineland, Phys. Rev. Lett. **76**, 1796 (1996).
[4] D. Leibfried, D. M. Meekhof, B. E. King, C. Monroe, W. M. Itano, and D. J. Wineland, Phys. Rev. Lett. **77**, 4281 (1996).
[5] C. Monroe, D. M. Meekhof, B. E. King, and D. J. Wineland, Science **272**, 1131 (1996).
[6] C. Monroe, D. M. Meekhof, B. E. King, W. M. Itano, and D. J. Wineland, Phys. Rev. Lett. **75**, 4714 (1995).
[7] S. Wallentowitz and W. Vogel, Phys. Rev. Lett. **75**, 2932 (1995).
[8] J. F. Poyatos, R. Walser, J. I. Cirac, and P. Zoller, Phys. Rev. A **53**, R1966 (1996).
[9] C. D'Helon and G. J. Milburn, Phys. Rev. A **52**, 4755 (1995).
[10] R. L. de Matos Filho and W. Vogel, Phys. Rev. Lett. **76**, 4520 (1996).
[11] P. J. Bardroff, C. Leichtle, G. Schrade, and W. P. Schleich, Phys. Rev. Lett. **77**, 2198 (1996); G. Schrade, P. J. Bardroff, R. J. Glauber, C. Leichtle, V. Yakovlev, and W. P. Schleich, Appl. Phys. B **64**, 181 (1997).
[12] J. F. Poyatos, J. I. Cirac, and P. Zoller, Phys. Rev. Lett. **77**, 4728 (1996).
[13] S. Wallentowitz, R. L. de Matos Filho, and W. Vogel, Phys. Rev. A **56**, 1205 (1997).
[14] D. T. Pegg and S. M. Barnett, Phys. Rev. A **39**, 1665 (1989).
[15] S. M. Barnett and D. T. Pegg, Phys. Rev. Lett. **76**, 4148 (1996).
[16] P. Figurny, A. Orlowski, and K. Wódkiewicz, Phys. Rev. A **47**, 5151 (1993).
[17] S. A. Gardiner, J. I. Cirac, and P. Zoller, Phys. Rev. A **55**, 1683 (1997).
[18] C. A. Blockey, D. F. Walls, and H. Risken, Europhys. Lett. **17**, 509 (1992).
[19] C. K. Law and J. H. Eberly, Phys. Rev. Lett. **76**, 1055 (1996).
[20] W. Vogel and R. L. de Matos Filho, Phys. Rev. A **52**, 4214 (1995).
[21] D. M. Greenberger, M. A. Horne, A. Shimony, and A. Zeilinger, Am. J. Phys. **58**, 1131 (1990); D. M. Greenberger, M. A. Horne, and A. Zeilinger, Phys. Today **46** (8), 22 (1993).
[22] The slight changes to the scheme due to a standing-wave configuration were shown in Ref. [17].
[23] F. Diedrich, J. C. Bergquist, W. M. Itano, and D. J. Wineland, Phys. Rev. Lett. **62**, 403 (1989); D. M. Meekhof, B. E. King, S. R. Jefferts, W. M. Itano, D. J. Wineland, and P. Gould, *ibid.* **75**, 4011 (1995).
[24] The validity of this approximation for the arbitrary state preparation method was discussed in Ref. [17].
[25] Our scheme is applicable for every Hamiltonian of this form. Therefore arbitrary state preparation is even possible in the time-dependent Paul trap potential beyond the secular approximation, as can be seen with the derivation in Ref. [11], where the micromotion is taken into account.
[26] U. W. Hochstrasser, in *Handbook of Mathematical Functions*, edited by M. Abramowitz and I. A. Stegun (Dover, New York, 1965), Chap. 22.
[27] In the nonentanglement case $\alpha=0$, we have $C_M=1$.
[28] Recognize that we always obtain solutions $|c_j|\tau$ and $|r_j|\tau$. Thus there is also the possibility to have constant electric fields $\mathcal{E}_j^{c,r}=\mathcal{E}^{c,r}$ for each pulse, and to adjust the time τ_j. Therefore the time of preparation can be optimized; see Ref. [19].
[29] It is obvious that Eqs. (21) and (22) always have a solution, since the right-hand side can be chosen to be real by adjusting the phases θ_j^c and θ_j^r, respectively. In fact there is always more than one solution because the inverse function of $\tan(x)$ has an infinite amount of branches.
[30] A π pulse is actually a $\pi/2$ pulse in our notation, as we defined the Rabi frequency to be periodical with 2π, and not with 4π.
[31] In the Lamb-Dicke regime, where the Rabi frequencies c_n associated with the carrier frequency channel become automatically independent of n, one can even use always the same field amplitude $\mathcal{E}_j^c=\mathcal{E}^c$ and time $\tau_j=\tau$ for that laser.
[32] F. A. M. de Oliveira, M. S. Kim, P. L. Knight, and V. Bužek, Phys. Rev. A **41**, 2645 (1990), and references therein.
[33] C. K. Law, J. H. Eberly, and B. Kneer, in *Quantum State Preparation and Measurement*, edited by W. P. Schleich and M. G. Raymer, special issue J. Mod. Opt. **44**, 2149 (1997).